Journal of Applied Electrochemistry **31**: 49–56, 2001.

Synthesis and characterization of polypyrrole/TiO_2 composites on mild steel

C.A. FERREIRA[1]*, S.C. DOMENECH[1] and P.C. LACAZE[2]
[1]*LAPOL–PPGEM, Universidade Federal do Rio Grande do Sul, Av. Osvaldo Aranha, 99 sala 702, 90035-190, Porto Alegre, Brazil*
[2]*ITODYS, Université Paris 7 Denis Diderot, 1, rue Guy de la Brosse, 75005, Paris, France*
*(*author for correspondence)*

Received 21 July 1998; accepted in revised form 9 July 2000

Key words: composites, electropolymerization, mild steel, polypyrrole, TiO_2

Abstract

The anodic codeposition of polypyrrole and TiO_2 on AISI 1010 steel substrates in oxalic acid medium was studied from the standpoint of their use as protective coatings against corrosion. The influence of surface treatment, pH, stirring and current density (j) on the current efficiency (γ) and pigment concentration incorporated in the polymer (C_c) were investigated. The highest C_c values (7.5%) were found at $j = 5$ mA cm^{-2}, pH 4 and stirred baths. The composites were characterized by adherence and surface roughness tests, XPS, EDX, SEM, FTIR and cyclic voltammetry.

1. Introduction

An improvement over conventional methods of industrially painting metal substrates was achieved with the introduction of the direct electropolymerization of aromatic monomers. The importance of the method is based on the unique properties of the electrical process. In principle, instead of starting with prefabricated waterborne polymers, it is interesting to use appropriate monomers, which form films by electropolymerization. The electrodeposition of synthetic metals like polypyrrole (PPy) on inert substrates such as Pt, Au, glassy carbon or stainless steel is possible under a wide variety of conditions and yields coatings which can be peeled off from the substrate for subsequent study of the material [1, 2]. However, oxidizable metals like Al, Cu, Zn, Fe and mild steel undergo severe anodic dissolution under the usual electrodeposition conditions of PPy.

In the specific case of mild steel, only a few systems allow the formation of a passive coating on the metal surface, which diminishes the corrosion of the substrate, and promotes the formation of polymer films: THF, CH_3OH with quaternary ammonium salts [4–6], aqueous nitrate [3–5] and aqueous oxalic acid [7]. Aqueous electrolytes are preferable from a practical point of view.

A possible application of these coatings as corrosion-inhibiting interlayers can be envisaged since the materials are insoluble in all solvents and the heterocyclic monomer units have the same structures as many known corrosion inhibitors [3, 7]. However, such an application depends on the achievement of strong adhesion of the polymer layer, typically 0.1–30 μm thick. It was found that adhesion is extremely good with the previously mentioned oxalate system on steel pretreated with manganese salts [7].

In our case, it was found that very adherent PPy films could be deposited on steel when its surface was treated by dilute HNO_3 [5, 8, 9]. This acid treatment allowed PPy layers to be obtained which could be reduced in NaOH and finally coated with a cataphoretic primer without disbonding, and which showed corrosion resistance (salt spray test) as good as the phosphate/cataphoretic system [5].

Electropolymerization has been used for the anodic deposition of synthetic metals like polypyrrole and dispersed solids on inert substrates [10–16]. In the case of oxide particle incorporation, however, there are some limitations. It was reported that oxide incorporation into a polypyrrole matrix electrodeposited on Pt or other noble metals is possible for metal oxides having relatively small values of the point of zero charges (p.z.c.) such as WO_3 and SiO_2 whose p.z.c. is at pH 0.5 and pH 2, respectively [10, 15]. Oxide particles are incorporated during the electrolysis of pyrrole in aqueous oxide suspensions by making the pH greater than the p.z.c. of the oxide, in order to produce negatively charged particles.

However, in the case of metal oxides such as TiO_2, whose p.z.c. is at pH 6.5, incorporation into the polymer matrix is only possible when small amounts of supporting electrolyte, whose anions specifically adsorb on TiO_2 particles, are added [15] or by electrosynthesis under strong stirring [16]. It was reported that the maximum amount of TiO_2 incorporated in the PPy matrix was

approximately 0.44 wt % in the first case and 17 wt % in the second, which suggests that oxide incorporation is markedly influenced by the synthesis conditions.

In this work, PPy/TiO_2 composites are synthesized on mild steel substrates with the aim of producing corrosion inhibiting interlayers. The expected role of the TiO_2 particles is to increase the barrier effect of the polymer matrix, improving its protecting properties. The process is proposed as an alternative to the usual systems of metal surface conditioning, such as phosphating, promoting better adherence of subsequent paint coatings.

2. Experimental details

The electrolyte used was oxalic acid (Synth) and the pH was adjusted by addition of NaOH (Synth). Pyrrole (Aldrich) was bidistilled under nitrogen just before use. All chemicals were analytical grade and the solvent was distilled water.

The pigment was TiO_2 (R-902, Du Pont) with a particle diameter of 0.2 μm, 91 $\pm$ 0.1% TiO_2 content. The TiO_2 (200 mg dm^{-3}) added to the electrolyte containing the monomer was stirred to promote dispersion for 30 min before electrodeposition.

The working electrode consisted of AISI 1010 steel (low carbon content), with an uncoated surface area of 16 cm^2. The pretreatment methods were: (A) alkaline degreasing (Duroclean 107, 80 °C, 10 min), acid etching (HCl 30 g dm^{-3} containing butynediol 1 g dm^{-3}, 25 °C, 10 min), wet grinding (240, 320, 400, 600), degreasing (C_2Cl_4) [7] and (B) alkaline degreasing (Duroclean 107, 80 °C, 10 min), acid etching (HNO_3) 10%, 25 °C, 5 min) [4].

The working electrode was placed between two counter-electrodes consisting of 0.1 cm thick SAE 304 stainless steel sheets (surface area 40 cm^2) 2 cm from each other. A potassium-saturated calomel electrode (SCE) was used as reference.

A PAR 273A (EG&G) potentiostat/galvanostat, connected to a PC was used and all the experiments were performed at room temperature (20 $\pm$ 5 °C) for 30 min. After electrosynthesis, the electrodes were thoroughly rinsed with distilled water, then dried at 40 °C for 1 h.

The electrosynthesis of PPy films proceeds at an anodically polarized electrode surface, according to the classical scheme:

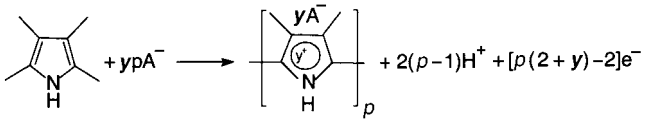

(1)

where y is the degree of insertion of the anions, corresponding to the degree of oxidation of the monomer units. The theoretical electrochemical equivalent ($m_{e,th}$), the current efficiency of the electropolymerization process (γ), the nominal thickness (d_n), as well as the real thickness of the polymer composites (d), are derived from this equation and were calculated by the method described in the literature [3–5].

The pigment concentration in the polymer matrix was determined as follows. The PPy/TiO_2 composite films were treated with hot concentrated HNO_3 to destroy the organic material. After evaporation of the acid, the product was dissolved in hot concentrated H_2SO_4 containing $(NH_4)_2SO_4$. The TiO_2 concentration was determined by using an ARL 3520B ICP analyser at 336.12 nm [17].

The adherence tests were performed as described elsewhere [20].

The average roughness depths R_a and R_z of the PPy and PPy/TiO_2 surfaces were measured with a commercial mechanical profilometer S6P-Perthen Mahr Perthometer. R_z is the average of five individual roughness depths, measured along five single lines, typically l = 0.8 mm. ΔR is the difference between the highest and the lowest peaks. R_z is defined as

$$R_z = \frac{l}{n\sum_{i=1}^{n}\Delta R_i} \quad (n = 5) \tag{2}$$

The mean roughness, R_a, averages all roughness elongations starting from an averaged straight line, where the microelongations rise in positive and negative directions. A total of three measurements were performed on the same specimen along a line about 5.6 mm long at various locations on the polymer surface.

Surface analysis was performed using a VG MK1 XPS spectrometer with a nonmonochromatic Mg source (K_α 1253.6 eV). These analyses were conducted at 10^{-8} mbar and the energies read in the spectra were referred to C1s at 285 eV.

Morphological aspects and elementary analysis were studied simultaneously with a Noran Instruments EDX system (energy dispersive X-ray analysis) connected to a Jeol JSM 6300 F scanning electron microscope. IR analysis was carried out with a Shimadzu FTIR 8121 spectrophotometer.

The corrosion resistance of the PPy films was estimated by measuring the corrosion potential (E_{corr}) of the electrodes immersed in a 3.5% NaCl solution for 120 h with an ET 2700 Minipa multimeter. Prior to experiments the polymer films were dedoped in a NaOH 0.5 M aqueous solution and at the same time a reduction potential of −0.5 V vs SCE was applied for 2 min.

3. Results

3.1. *Electrodeposition of PPy films on AISI 1010 steel*

The electropolymerization of PPy coatings in the absence of TiO_2 was performed in order to observe the influence of the current density (5 and 10 mA cm^{-2}), pH

(2 and 4), stirring and surface pre-treatment on the current efficiency (γ) of the process. All the galvanostatic experiments were carried out in a 0.1 M oxalic acid and 0.1 M pyrrole solution (thereafter called oxalic acid/pyrrole solution).

According to Table 1, current efficiency reaches a maximum value (γ = 65.6%) for the following conditions (sample 1): j = 5 mA cm^{-2}, pH 2, no stirring and surface pretreatment B (HNO_3 etching). Current efficiency drops from 65.6% to 57.0% at pH 4 (sample 9).

Magnetic stirring of the electrolyte reduces current efficiency, as seen, for example, in the marked decrease from 65.6% to 9.9% (by using surface pretreatment B) and from 26.5% to 3.2% (pretreatment A) in experiments conducted at 5 mA cm^{-2} , and pH 2 (Table 1).

In less acidic solutions, the current efficiency (γ) decreases for almost all experiments, as can be seen in Table 1 comparing samples 1 to 8 (pH 2) with samples 9 to 16 (pH 4). Due to proton generation during electropolymerization (Equation 1) the diffusion layer becomes acidic, and prevents the nucleophilic attack of OH^- ions from the reduction of water at the cathode. Schirmeisen and coworkers [6] observed that, in aqueous acidic solutions, marked dissolution of the substrate occurred, whereas in alkaline solutions inorganic coatings with strong adherence to the substrate were formed and impeded the electrosynthesis. The real thickness (d) of the films varied between 19.0 and 0.6 μm, according to the different synthesis conditions (Table 1).

PPy films were formed at substrates pretreated either by method A or B but with marked differences in the current efficiency and adherence. The highest values of γ and the stronger adherence were obtained with steel substrates pretreated by method B (HNO_3 etching).

Current efficiency decreased with increase in applied current density from 5 to 10 mA cm^{-2}, even at different pH. This behaviour was more evident in experiments carried out without stirring for 30 min, as described in Figure 1.

Table 1. Current efficiencies (γ), nominal (d_n) and real (d) thickness for the synthesis of PPy on mild steel in the pyrrole/oxalic acid solution

Sample	j/mA cm^{-2}	pH	Stirring (Y/N)	Surface treatment (A/B)	γ/%	d_n/μm	d/μm
1	5	2	N	B	65.6	23.9	15.6
2	10	2	N	B	39.8	47.8	19.0
3	5	2	Y	B	9.9	23.5	2.3
4	10	2	Y	B	5.9	49.1	2.9
5	5	2	N	A	26.5	24.8	6.6
6	10	2	N	A	11.9	50.5	6.0
7	5	2	Y	A	3.2	25.0	0.8
8	10	2	Y	A	5.4	50.5	2.7
9	5	4	N	B	57.0	24.3	13.8
10	10	4	N	B	38.9	48.1	18.7
11	5	4	Y	B	9.8	21.0	2.1
12	10	4	Y	B	2.4	48.2	1.2
13	5	4	N	A	17.5	24.8	4.3
14	10	4	N	A	13.1	50.1	6.5
15	5	4	Y	A	4.6	24.6	1.1
16	10	4	Y	A	1.1	50.5	0.6

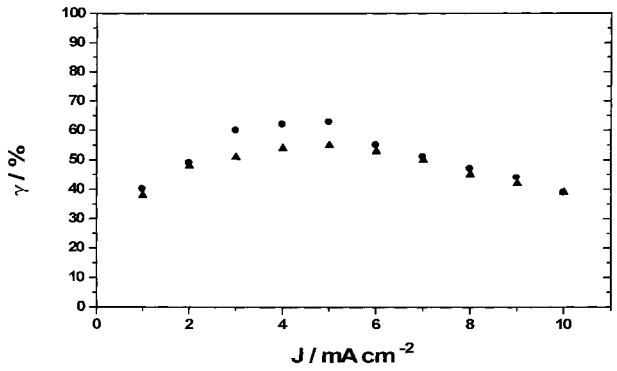

Fig. 1. Influence of the current density (j) on the current efficiency (γ) of PPy films synthesized on AISI 1010 steel. Synthesis conditions: pyrrole/oxalic acid solution, without stirring. Surface pretreatment B. Key: (●) pH 2 and (▲) pH 4.

The current efficiency increases with increase in applied current density from 1 to 5 mA cm^{-2}, reaching a maximum value of 65.6% at 5 mA cm^{-2} (Figure 1). Such behaviour was also observed by other authors [3, 5–7] who studied the electrodeposition of PPy using different electrolytes and anodes. The decrease of γ at j > 5 mA cm^{-2} is related to overoxidation reactions of the polymer layer, which leads to the release of products soluble in the electrolyte solution [21].

The electrosynthesis curves of PPy (Figures 2 and 3) show an induction period related to the dissolution of the steel substrate. The induction time decreases with increasing current density, and is practically zero at density current 5 mA cm^{-2}, which explains the increase in current efficiency when the current density increases from 1 to 5 mA cm^{-2}. When the applied current density varies from 5 to 10 mA cm^{-2}, the potential values increase dramatically up to 7.5 V vs SCE at 10 mA cm^{-2}, inducing overoxidation of the polymer layer.

3.2. *Electrodeposition of PPy/TiO_2 films on AISI 1010 steel*

The experiments were run on the oxalic acid/pyrrole solution containing TiO_2 (200 mg dm^{-3}). The current

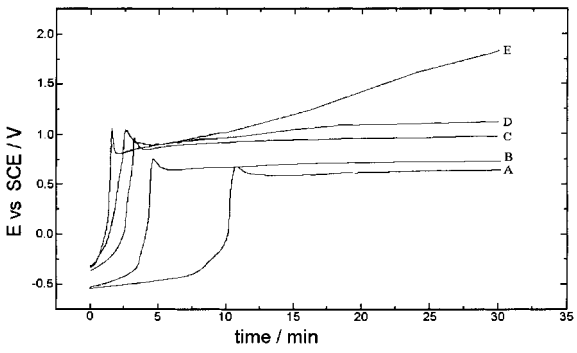

Fig. 2. Potential against time curves for the galvanostatic electrodeposition of PPy on AISI 1010 steel. Synthesis conditions: pyrrole/oxalic acid solution. Surface pretreatment B. A, B, C, D, E = 1, 2, 3, 4, 5 mA cm^{-2}, respectively.

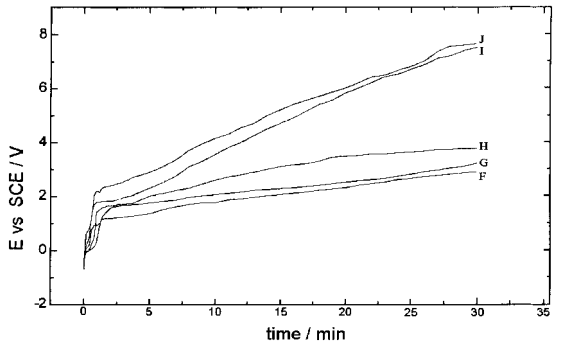

Fig. 3. Potential against time curves for the galvanostatic electrodeposition of PPy on AISI 1010 steel. Synthesis conditions: the same as previously. Surface pretreatment B. F, G, H, I and $J = 6$, 7, 8, 9 and 10 mA cm^{-2}, respectively.

efficiencies (γ) of the electropolymerization process, the TiO_2 concentration incorporated in the composite (C_c) as well as the nominal (d_n) and the real thickness of the polymer films (d) are described in Table 2.

Electrosynthesis carried out in the presence of TiO_2 gives lower current efficiencies than electropolymerization of pyrrole alone (Table 1). Maximum values of γ (44.7%) were reached with experiments at pH 2, 5 mA cm^{-2}, with no stirring and by using surface pretreatment B.

Again, a decrease in γ (23.0%) is observed at pH 4. Magnetic stirring and the use of pretreatment A causes a decrease in current efficiency. Moreover, current efficiency increases as j varies from 1 to 5 mA cm^{-2} and decreases from 5 to 10 mA cm^{-2}, in a similar way to experiments shown in Figure 1 and conducted without TiO_2.

The highest value of TiO_2 incorporation in the polymer matrix is 7.5% and was obtained with magnetic stirring, suggesting that stirring improves the stability of the suspension. The higher incorporation of TiO_2 at pH 4 is probably due to the fact that the pigment particles acquire negative charges, as reported by Yoneyama [14].

3.3. *Characterization of PPy/TiO_2 composites*

3.3.1. *Adherence strength*

Both PPy films and PPy/TiO_2 film composites were obtained under the same conditions as in Tables 1 and 2.

Table 2. Current efficiencies (γ), TiO_2 concentration in the composite (C_c), nominal (d_n) and real (d) thickness for the synthesis of PPy on mild steel in the pyrrole/oxalic acid solution containing 200 mg dm^{-3} of TiO_2

Sample	j/mA cm^{-2}	pH	Stirring (Y/N)	Surface treatment (A/B)	γ/%	C_c/%	d_n/μm	d/μm
17	5	2	N	B	44.7	2.7	23.5	10.5
18	10	2	N	B	25.8	1.1	49.8	12.8
19	5	2	Y	B	10.6	4.1	23.6	2.5
20	10	2	Y	B	10.9	2.9	49.2	5.4
21	5	2	N	A	26.8	2.0	24.9	6.7
22	10	2	N	A	16.2	0.4	50.3	8.2
23	5	2	Y	A	5.3	2.3	24.9	1.3
24	10	2	Y	A	12.6	0.3	50.1	6.3
25	5	4	N	B	23.0	7.0	21.6	4.9
26	10	4	N	B	12.3	2.2	46.9	5.7
27	5	4	Y	B	1.0	7.5	19.1	0.2
28	10	4	Y	B	3.3	3.0	45.2	1.5
29	5	4	N	A	17.9	6.9	24.9	4.5
30	10	4	N	A	5.3	0.4	50.2	2.6
31	5	4	Y	A	2.2	7.2	24.6	0.5
32	10	4	Y	A	2.4	0.3	50.2	1.2

It was observed that the use of surface treatment B (HNO_3 etching) allowed the formation of PPy coatings with 100% adherence. These results depended neither on the pH of the solution nor on the applied current density. With samples pretreated by method A (HCl etching) adherence to the metal substrate was low and ranged from 0 to 50%.

In the case of PPy/TiO_2 composites pretreatment B was not as good as for PPy alone and yielded PPy/TiO_2 films with adherence ranging from 75 to 100%. Treatment A was still poorer and gave 0–25% adherence.

3.3.2. *Surface roughness*

Surface roughness tests (Table 3) were done on steel substrates pre-treated by methods A and B as well as on PPy and PPy/TiO_2 films. Figure 4 shows the surface roughness profiles of bare steel samples after pretreatment, as well as the surface roughness profiles for steel surfaces coated by PPy and PPy/TiO_2 composites.

It was observed that the steel samples submitted to pretreatment A presented lower R_a and R_z values than those pretreated by method B (Table 3). The PPy films

Table 3. Surface roughness data for bare steel, PPy and PPy/TiO_2 coatings

Synthesis conditions	Surface pretreatment	d_n/μm	Surface roughness Parameter/μm	Analysed surface		
				AISI 1010 steel	PPy	PPy/TiO_2
Sample 2	B	47.8	R_a	6.5	7.1	
Table 1			R_z	33.8	36.0	
Sample 7	A	25.0	R_a	0.5	0.58	
Table 1			R_z	4.1	3.72	
Sample 18	B	49.8	R_a	4.3		9.5
Table 2			R_z	24.8		50.4
Sample 23	A	24.9	R_a	1.1		2.9
Table 2			R_z	5.8		18.6

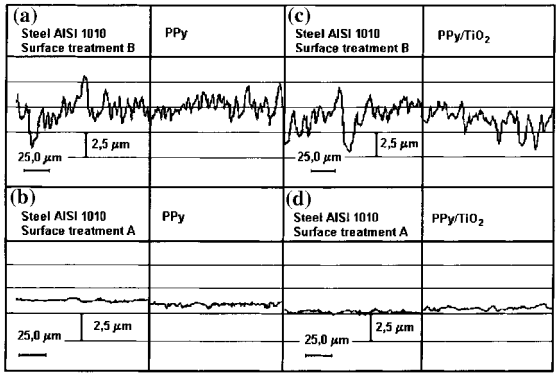

Fig. 4. Surface profiles of bare steel, steel + PPy and steel + PPy/TiO_2. Synthesis conditions: (a) and (b) oxalic acid/pyrrole solution. (c) and (d) oxalic acid/pyrrole solution + TiO_2 200 mg dm^{-3}, j = 5 mA cm^{-2}, no stirring, pH 4.

deposited on surfaces pretreated by method A presented lower values of average roughness than those where method B was employed.

From Table 3 and Figure 4, we perceive a leveling effect of the metallic surfaces with PPy films and this effect is stronger in the case of the PPy/TiO_2 composites.

3.3.3. *XPS analysis*

A 10 μm PPy/TiO_2 composite was deposited on a steel sample pretreated by alkaline degreasing. After the electrodeposition experiment, the film was detached from the substrate. XPS analysis was performed on the steel surface, on the internal face of the composite (which was in contact with the metal surface) and the outer PPy/TiO_2 layer. This analysis was intended to obtain information about pigment localization and also to identify the substances formed on the surfaces.

On the whole, the XPS spectra of the PPy/TiO_2 spectra are similar to those reported in the literature [3, 4, 8, 21–23]. Analysis of the outer face of the PPy/TiO_2 film shows two peaks at 534.4 eV and at 532 eV (signal O1s) associated with oxygenated organic compounds. The typical peak of ferrous oxides at 530 eV (signal $Fe2p_{3/2}$) is missing. The N1s signal consists of two peaks, at 400 and 402 eV, corresponding to the pyrrole ring and to partially charged pyrrole, respectively. The C1s peaks at 288.8 and 286.7 eV are due to C═O and C—O groups, respectively, and the peak at 285 eV to the C—C groups of the polymer chain. Ti and Fe were not detected.

XPS analysis of the inner face of the composite film also showed O1s, N1s and C1s signals. The O1s consisted of three components at 535.6, 533.3 and 531 eV, associated with oxygenated organic compounds. The N1s signal presented one peak at 400 eV, typical of a neutral pyrrole ring. Deconvolution of the C1s signal into five peaks confirms the presence of oxalate at 292.3 eV, the presence of COOH, C═O and C—O groups at 290.4, 288.4 and 286.4 eV, respectively, and the presence of C—C groups of the polymer chain at 285 eV. Again, Ti and Fe were not detected.

The steel surface shows two peaks at 727.6 and 724 eV ($Fe2p_{1/2}$ signal) and two peaks at 714 and 710.9 eV related to ferrous oxides. The C1s signal shows one peak with binding energy of 288 eV attributed to oxygenated organic compounds (C═O groups) and another strong peak at 285 eV corresponding to C—C groups, which can be related to the presence of iron oxalate formed on the metal surface.

The failure to detect Ti by this technique indicates that the pigment particles are not located on the polymer surface or on the metal surface, but inside the film. The XPS results show that the composite film does not present ferrous oxides at its surface, and indicates that the metallic surface is fully covered by a nonporous polymer film.

3.3.4. *EDX elemental analysis and morphology*

The morphology of the PPy films and the PPy/TiO_2 composites was observed by SEM. EDX analysis was also performed to confirm the incorporation of the pigment in the polymeric material. The elements analysed were Ti, Al, Si and Na. The spectra were obtained at 200× magnification.

Ti was detected in all PPy/TiO_2 samples which confirms that the pigment is located inside the film and not at its surface (Figure 5). The absence of Al and Si indicates that the pigment is not treated with SiO_2 or Al_2O_3 during the fabrication process. The presence of Na in some samples probably comes from the NaOH solution, which was used to adjust the pH of the electrolyte.

Figure 6 shows the SEM micrographs of PPy and PPy/TiO_2 films obtained under conditions described in Tables 1 and 2.

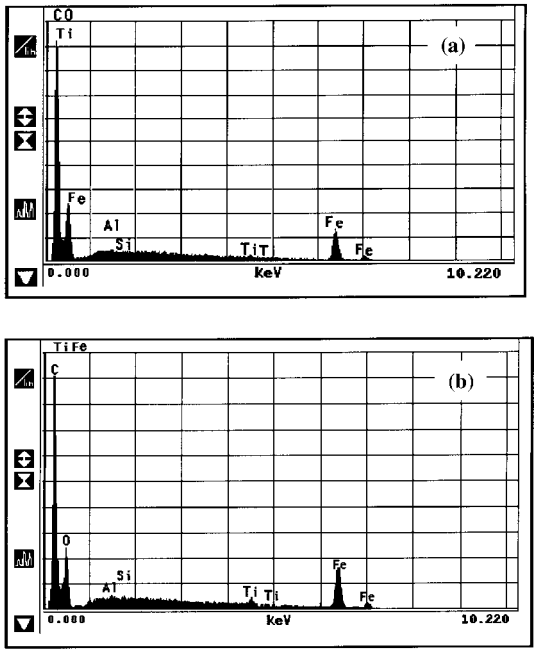

Fig. 5. EDX spectra of the polymer films obtained on AISI 1010 steel. (a) PPy. (b) PPy/TiO_2. Synthesis conditions: j = 5 mA cm^{-2}, pH 2, no stirring, pretreatment B.

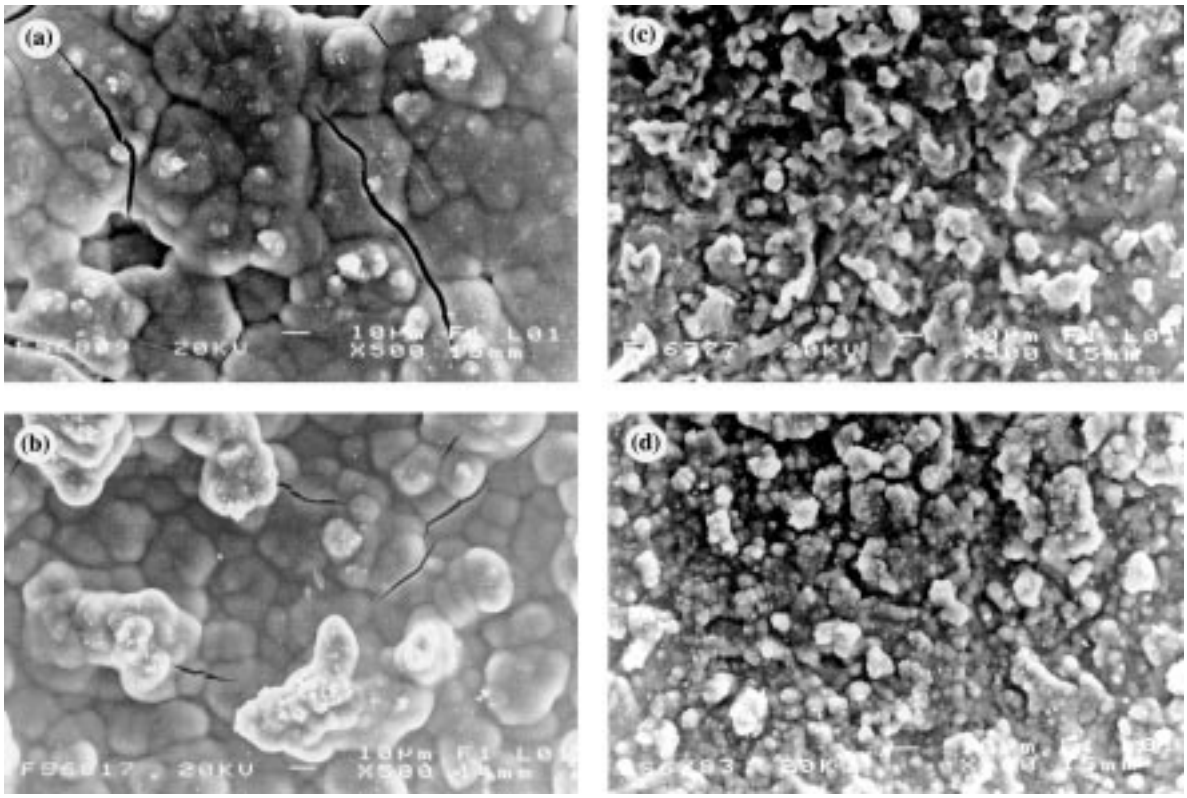

Fig. 6. SEM micrographs for PPy and PPy/TiO_2 on AISI 1010 steel. Synthesis conditions: oxalic acid/pyrrole solution + TiO_2 200 mg dm^{-3}, no stirring, pretreatment B. (a) $j = 5$ mA cm^{-2}, pH 2; (b) $j = 10$ mA cm^{-2}, pH 2; (c) $j = 5$ mA cm^{-2}, pH 4; (d) $j = 10$ mA cm^{-2}, pH 4.

The PPy/TiO_2 composites show the cauliflower morphology typical of PPy films electrochemically synthesized with $H_2C_2O_4$ [7, 23], KNO_3 [4], Na_2SO_4 [24], as well as PPy/WO_3 [11, 12] and PPy/TiO_2 composites [15, 16] deposited on Pt.

Generally, it was observed that the composites are nonporous and form compact films on the steel surfaces. However, the presence of some defects at the surface was noted and, in particular, with films synthesized at pH 2 (Figure 6(a) and (b)). As mentioned previously, the surface roughness of the PPy/TiO_2 composites is higher than those of the PPy films, which suggests that the incorporation of the pigment particles occurs by mechanical bonding and that this is governed by the number of surface defects as described by Beck et al. [16].

3.3.5. *FTIR analysis*

Figures 7 and 8 show the FTIR spectra of a PPy film and a PPy/TiO_2 composite obtained under the same conditions.

The main typical absorption bands of PPy were found in both spectra and confirm that both present the same characteristic chemical PPy structure. In particular, the C—H out-of-plane vibrations bands of medium intensity at 781 and 906 cm^{-1}, accompanied by the C—H in plane vibration bands at about 1045–1187 cm^{-1}. The N—H deformation band arises at approximately 1031–1032 cm^{-1} and the deformation of the pyrrole ring (C=C stretching) is well identified at 1375 cm^{-1}.

The peaks observed at 1623–1655 cm^{-1} in the case of PPy (Figure 8) are related to C=O band due to defects (pyrrolidinone).

3.3.6. *Cyclic voltammetry*

The electrochemical behaviour of PPy films (Figure 9) and Ppy/TiO_2 composites (Figure 10) was studied by cyclic voltammetry. The experiments were performed in aqueous 1 M $LiClO_4$ and at a scan rate of 2 mV s^{-1}.

The polymer films show electrochemical activity, with classical oxidation-reduction peaks of PPy. The voltammograms of the PPy/TiO_2 films have practically the same characteristics as those of the PPy, but the areas of the oxidation and reduction peaks are smaller.

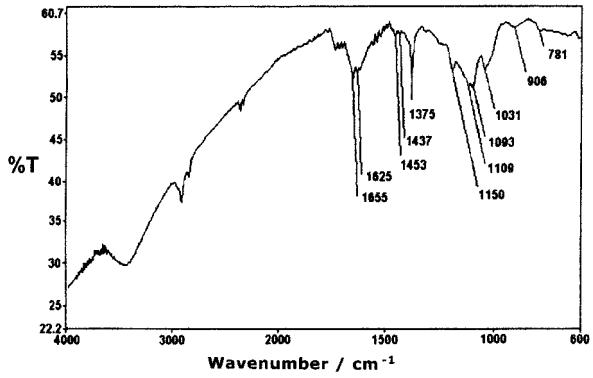

Fig. 7. FTIR spectra of PPy film. Synthesis conditions: oxalic acid/pyrrole solution, pH 2, $j = 5$ mA cm^{-2}.

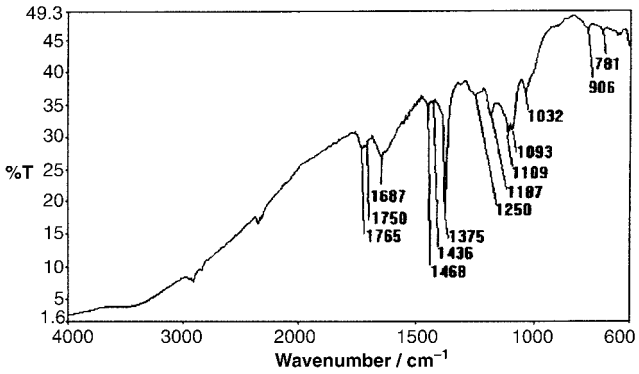

Fig. 8. FTIR spectra of PPy/TiO_2 film. Synthesis conditions: same as Figure 7, except the addition of 200 mg dm^{-3}.

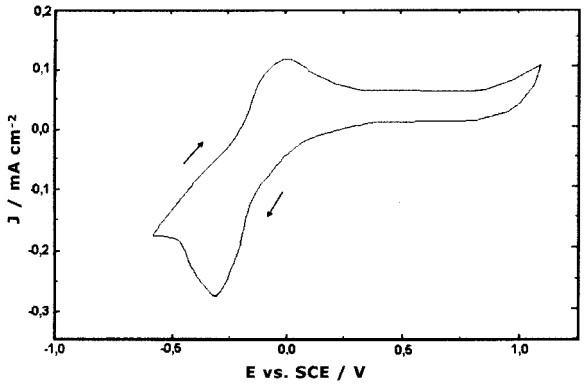

Fig. 9. Cyclic voltammetry of PPy film in 1 M $LiClO_4$ solution, without stirring, $v = 2$ mV s^{-1}. Synthesis conditions: oxalic acid/pyrrole solution, pH 4, $j = 5$ mA cm^{-2}.

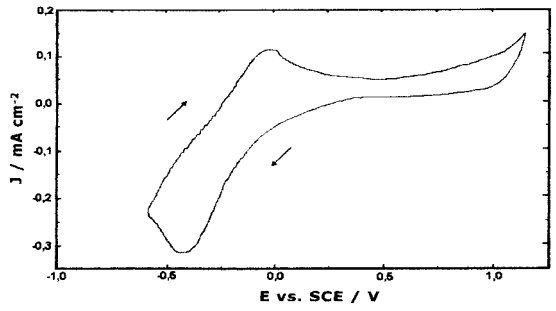

Fig. 10. Cyclic voltammetry of PPy/TiO_2 composite film in 1 M $LiClO_4$ solution, without stirring, $v = 2$ mV s^{-1}. Synthesis conditions: oxalic acid/pyrrole solution, pH 4, $j = 5$ mA cm^{-2}.

3.3.7. *Corrosion tests*

The corrosion resistance of the PPy films and PPy/TiO_2 composites was observed by immersion of the steel samples coated by polymer films in 3.5% NaCl solution. The equilibrium corrosion potential (E_{corr}) of the systems was measured and plotted as shown in Figure 11.

The initial corrosion potential of the composite was more anodic than for PPy films. The first points of corrosion (rust) were observed after 5 h immersion of PPy films and after 11 h for the composites. Figure 11 shows that the specimens coated with PPy/TiO_2 films

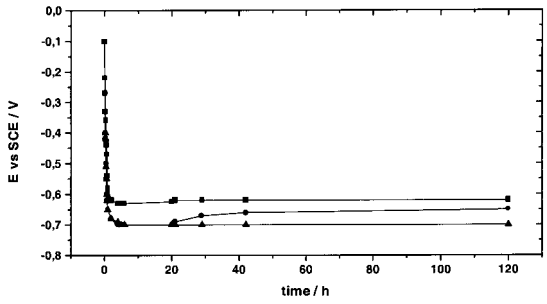

Fig. 11. Corrosion potential against time curves of AISI 1010 steel in 3.5% NaCl solutions. Key: (▲) bare steel, (●) steel + PPy and (■) steel + PPy/TiO_2 composite film.

exhibited higher E_{corr} (i.e., more noble) than those coated with PPy films or the bare steel substrate. After 120 h of immersion, the corrosion potential difference between uncoated steel and PPy films and PPy/TiO_2 composites was 50 and 70 mV, respectively, in accordance with other results described previously for similar mild steel but coated with polyaniline [25].

4. Conclusions

Several reaction conditions influence the galvanostatic electropolymerization of pyrrole on AISI 1010 steel in a 0.1 M $H_2C_2O_4$ + 0.1 M pyrrole solution: the highest current efficiency γ (65.6%) was obtained at pH 2, at 5 mA cm^{-2}, without stirring and using the HNO_3 etching (pretreatment B). The induction period related to the dissolution of the substrate decreases with increasing current density but when $j > 5$ mA cm^{-2} the measured potential increases dramatically inducing overoxidation of the polymer layer. The synthesis of PPy/TiO_2 composite films exhibits lower current efficiency than the simple PPy layers produced in the absence of TiO_2. The highest values of TiO_2 incorporation in the polymer matrix were observed at pH 4 with magnetic stirring, which improves the stability of the suspension.

Surface treatment B, which allowed the formation of PPy films with 100% adherence, unaffected by the pH of the solution or by the applied current density, was not so efficient for PPy/TiO_2 composites (75–100% adherence). Pretreatment A was still poorer and yielded films with only 0–25% adherence, a result which could be due to the fact that pretreatment B, in contrast to treatment A, led to a strong roughness of the steel surface.

XPS results demonstrate that the composite films do not contain ferrous oxides. TiO_2 was not detected by this method, indicating that the pigment particles are located inside the film, as confirmed by EDX elemental analysis.

PPy/TiO_2 composites showed a cauliflower morphology, typical of electrochemically synthesized PPy films. The films formed on the metal surface were nonporous, compact and a leveling effect was observed.

FTIR spectra demonstrated that there are no significant chemical structure differences between PPy and Ppy/TiO_2 film composites.

PPy/TiO_2 films give a more anodic corrosion potential than PPy or steel substrates, suggesting that the presence of the pigment improves the protective properties of the films.

The electrodeposition of PPy/TiO_2 composites on mild steel with high current efficiencies and with high TiO_2 concentration depends on the synthesis conditions. Synthesis in oxalic acid medium has some advantages, such as low cost, simplicity of the method and the absence of organic solvents. Composites formed with conducting polymers and TiO_2 are proposed as an alternative material for the preparation of mild steel surfaces previous to the application of the painting system.

Acknowledgements

Financial support by CAPES is gratefully acknowledged. We are obliged to VARIG S/A for the TiO_2 analysis, ALBARUS TH for the roughness profile tests, to Tintas Renner S/A for providing the TiO_2 pigment, to M. Zimnol (Max-Planck Institut – Germany) for performing the MEV–EDX elementary analysis and to Prof. M. Delamar (Université Paris 7, France) for XPS analysis.

References

1. A.F. Diaz, K.K. Kanazawa and G.P. Gardini, *J. Chem. Soc. Chem. Commun.* (1979) 635.
2. G.B. Street, *in* T.A. Skotheim (Ed), 'Handbook of Conducting Polymers', Vol. 1 (Marcel Dekker, New York, 1986), p. 265.
3. M. Schirmeisen and F. Beck, *J. Appl. Electrochem.* **19** (1989) 401.
4. C.A. Ferreira, S. Aeiyach, M. Delamar and P.C. Lacaze, *J. Electroanal. Chem.* **284** (1990) 351.
5. (a) C.A. Ferreira, PhD thesis, Université Paris 7 (1991); (b) C.A. Ferreira, S. Aeiyach, A. Coulaud and P.C. Lacaze, *J. Appl. Electrochem.* **29** (1999) 259.
6. C.A. Ferreira, S. Aeiyach, J.J. Aaron and P.C. Lacaze, *French patent* 2 698 379, 27 May (1994).
7. F. Beck and M. Michaelis, *J. Coat. Technol.* **64** (1992) 59.
8. C.A. Ferreira, S. Aeiyach, J.J. Aaron and P.C. Lacaze, *in* P.C. Lacaze (Ed), 'Organic Coatings', A.I.P. Conference Proceedings **354** (1996), p. 153.
9. C.A. Ferreira, S. Aeiyach, J.J. Aaron and P.C. Lacaze, *Electrochim. Acta* **41** (1996) 1801.
10. H. Yoneyama and Y. Shoji, *J. Electrochem. Soc.* **137** (1990) 3826.
11. F. Beck and M. Dahlhaus, *J. Appl. Electrochem.* **23** (1993) 781.
12. M. Dahlhaus and F. Beck, *J. Appl. Electrochem.* **23** (1993) 957.
13. G. Bidan, O. Jarjayes, J.M. Fruchart and E. Hannecart, *Adv. Mat.* **6** (1994) 152.
14. H. Yoneyama, M. Tokuda and S. Kuwabata, *Electrochim. Acta* **39** (1994) 1315.
15. K. Kawai, N. Mihara, S. Kuwabata and H. Yoneyama, *J. Electrochem. Soc.* **137** (1990) 1793.
16. F. Beck, M. Dahlhaus and N. Zahedi, *Electrochim. Acta* **37** (1992) 1265.
17. S.C. Domenech, Master of Science dissertation UFRGS, Brazil (1997).
18. Associação Brasileira de Normas Técnicas, ABNT P-MB-985 (1984).
19. Associação Brasileira de Normas Técnicas, NBR 6 (1988).
20. American Society for Testing Materials, ASTM D-870-54 (1980), p. 183.
21. P. Novak, B. Rasch and W. Vielstich, *J. Electrochem. Soc.* **138** (1991) 3300.
22. E.T. Kang, K.G. Neoh, Y.K. Ong, K.L. Tan and B.T.G. Tan, *Macromol.* **24** (1991) 2822.
23. V. Haase and F. Beck, *Electrochim. Acta* **39** (1994) 1195.
24. K.L. Tan, B.T.G. Tan, E.T. Kang, K.G. Neoh and K.G. Ong, *Phys. Rev.* **42** (1990) 7563.
25. Y. Wei, J. Wang, X. Jia and J-M. Yeh, *Polymer* **36** (1995) 4535.